Altered Amplitude of Low-Frequency Fluctuation in Primary Open-Angle Glaucoma: A Resting-State fMRI Study

Ting Li,[1] Zhenyu Liu,[2] Jianhong Li,[1] Zhaohui Liu,[1] Zhenchao Tang,[3] Xiaobin Xie,[4] Diya Yang,[5] Ningli Wang,[5] Jie Tian,[2,6] and Junfang Xian[1]

[1]Department of Radiology, Beijing Tongren Hospital, Capital Medical University, Beijing, China
[2]Key Laboratory of Molecular Imaging, Institute of Automation, Chinese Academy of Sciences, Beijing, China
[3]School of Mechanical, Electrical and Information Engineering, Shangdong University, Weihai, Shangdong, China
[4]Department of Ophthalmology, Eye Hospital of China Academy of Chinese Medical Sciences, Beijing, China
[5]Department of Ophthalmology, Beijing Tongren Hospital, Capital Medical University, Beijing, China
[6]School of Life Science and Technology, Xidian University, Xi'an, Shanxi, China

Correspondence: Jie Tian, Institute of Automation, Chinese Academy of Sciences, P.O. Box 2728, Beijing, 100190, China; tian@ieee.org.
Junfang Xian, Department of Radiology, Beijing Tongren Hospital, NO.1 of Dongjiaominxiang Street, Dongcheng District, Beijing, 100730, China; cjr.xianjunfang@vip.163.com.

TL and ZL contributed equally to the work presented here and should therefore be regarded as equivalent authors.

Submitted: June 7, 2014
Accepted: December 9, 2014

Citation: Li T, Liu Z, Li J, et al. Altered amplitude of low-frequency fluctuation in primary open-angle glaucoma: a resting-state fMRI study. *Invest Ophthalmol Vis Sci*. 2015;56:322–329. DOI:10.1167/iovs.14-14974

Purpose. To analyze the altered amplitude of low-frequency fluctuation (ALFF) of the brain using resting-state functional magnetic resonance imaging (fMRI) in patients with primary open-angle glaucoma (POAG).

Methods. Resting-state fMRI was conducted in 21 POAG patients and 22 age-matched healthy control subjects. After the ALFF and fractional amplitude of low-frequency fluctuation (fALFF) for slow 4 and slow 5 bands were calculated, the results between POAG patients and healthy controls were compared. Then the correlations between ALFF/fALFF values and the disease stage of POAG were analyzed.

Results. Compared with controls, POAG patients showed significantly decreased ALFF/fALFF values in the visual cortices, posterior regions of the default-mode network (DMN), and motor and sensory cortices. Meanwhile, ALFF/fALFF values in the prefrontal cortex, left superior temporal gyrus (STG), right middle cingulate cortex (MCC), and left inferior parietal lobule (IPL) significantly increased in POAG patients. Hodapp-Anderson-Parrish (HAP) score for POAG was positively correlated with ALFF values of the right superior frontal gyrus (SFG) and negatively correlated with that of the left cuneus. For the slow 5 band, the fALFF values of the bilateral middle temporal gyri (MTG) of POAG patients were negatively correlated with HAP score.

Conclusions. Primary open-angle glaucoma is a neurodegenerative disease involving multiple brain regions, including the visual cortices, DMN, limbic system, and motor and sensory networks. Moreover, the alterations in some of these networks are correlated with the progression of POAG; for the abnormal spontaneous neural activities in the left cuneus, bilateral MTG and right prefrontal cortex are correlated with glaucoma severity.

Keywords: functional magnetic resonance imaging (fMRI), resting state fMRI, primary open angle glaucoma, spontaneous activity

Primary open-angle glaucoma (POAG) is a type of progressive neuropathy with no clear cause, characterized by the loss of retinal ganglion cells (RGC).[1] It always begins in a silent way and slowly progresses to blindness.[2,3] It is predicted that glaucoma will affect 76.0 million people by 2020 and 111.8 million in 2040.[4]

At present, neurology and pathology research puts forward the theory that POAG is a neurodegenerative disease involving the brain,[5,6,7] and the pathologic mechanism in glaucoma is similar to that in Alzheimer's disease (AD).[8,9] Earlier research showed abnormalities in the primary visual cortex (PVA) in POAG.[7,10–12] Subsequent studies reported structural abnormalities extending into areas beyond the visual pathway.[13,14] These results suggest that POAG is not only a disease limited to the visual system, but also a neurodegenerative disease involving multiple brain regions. Functional magnetic resonance imaging (fMRI), which is widely used in various neurodegenerative diseases involving the central nervous system (CNS), is also appropriate for exploring the mechanism of POAG. With monocular visual stimulation, the attenuation of the blood oxygenation level dependent (BOLD) signal in the PVA is consistent with the visual defect in POAG patients.[15,16] Furthermore, Qing et al.[17] found that cortical depression is negatively correlated with pattern standard deviation in a visual field analysis. These task-related studies have helped in correlating the visual defect with alteration of brain function. Nonetheless, these results could not distinguish whether the abnormal activity in the brain is spontaneous or a response to the abnormal impulse introduced by the injured RGC. Spontaneous BOLD fluctuations of resting-state fMRI could reflect spontaneous neuronal activity.[18] A previous study has shown that nonrandom spontaneous activity exists in the PVA of waking adults, and it could be associated with memory-related mental imagery and visual memory consolidation processes.[19] In a resting-state fMRI study of POAG, Dai et al.[20] made the point that the functional connectivity between the

Table 1. Subject Characteristics

	POAG	Controls
N	21	22
Age range, y	17–75	24–65
Age, mean ± SD	46.4 ± 16.4	45.6 ± 11.9
Sex, M/F	10/11	11/11
Handedness, right/left	21/0	22/0
HAP score, mean ± SD	4.7 ± 2.2	0/0
Mean deviation, right/left	−13.6/−12.6	0/0
Mean IOP, right/left	17.8/17.7	12.3/13.1

Hodapp-Anderson-Parrish score is the summation of HAP grading scales of both eyes. IOP, intraoptic pressure.

visual cortex and the components of some resting-state networks is abnormal in patients with POAG. However, the alteration of spontaneous neural activity in POAG patients is still in need of further exploration.

Amplitude of low-frequency fluctuations (ALFF) represents the intensity of low-frequency oscillations (LFOs).[21] It has been proven to be a valuable parameter to reflect the intensity of spontaneous neural activity.[22] With a small difference, fractional ALFF (fALFF) is an index that reflects the relative contribution of specific LFOs to the entire frequency range. Previous neuroimaging results have indicated that fALFF could improve sensitivity and specificity in detecting abnormal brain activities.[23] In previous resting-state fMRI studies, spontaneous oscillation activities have been commonly examined at a frequency band of 0.01 to 0.1 Hz, which is considered to be linked to neuronal BOLD fluctuations.[18,24] However, the high frequency is for high-level interactions involving distant structures, while the low frequency is for relatively local area computation.[25] Meanwhile, several rhythms can temporally coexist in the same or different structures and interact with each other.[26] Thus, a combination of the two parameters can acquire more information about the brain with POAG and verify the abnormal functional activities reported before.

In the present study, the distribution of anomalous regional intrinsic activities in the glaucomatous brain was explored, and a correlation between the brain abnormalities and the severity of the disease was revealed. Considering that the pattern of intrinsic brain activity is sensitive to specific frequency bands,[27,28] we analyzed the changes in fALFF in the slow 5 band (0.01–0.027 Hz) and the slow 4 band (0.027–0.073 Hz) separately, and then compared the two results. We hypothesized that in patients with POAG, the abnormal spontaneous activities are not located only in the visual cortex but also in some other functional networks.

Materials and Methods

Subjects

Twenty-one POAG patients and 22 age-matched healthy control subjects were included in this study (see Table 1 for subjects' characteristics). There were no statistically significant differences in age and sex between the two groups ($P > 0.05$). After being given a complete description of the study, all subjects signed the informed consent form. All protocols were approved by a local subcommittee on human studies and in accordance with the Declaration of Helsinki.

Primary open-angle glaucoma patients were recruited at the Beijing Tongren Hospital, and the healthy subjects came from the local community. The patients were recruited into the study based on the clinical diagnostic criteria of POAG: a history of open anterior chamber angle, visual field defects, abnormal optic disc, and increased intraocular pressure. Subjects underwent a thorough history and physical examination including an ophthalmology examination. Inclusion criteria for the POAG group were (1) a clinical examination confirming POAG and (2) the presence of a visual field defect. Exclusion criteria for the POAG group included (1) clinical evidence or history of other oculopathy; (2) history of any significant medical, neurological, or psychiatric illness including hypertension and diabetes; and (3) use of alcohol, caffeine, or nicotine within the last 3 months. Inclusion criteria for the control group stipulated that they be healthy volunteers age and sex matched to the patient group without clinical evidence or history of glaucoma. Exclusion criteria were (1) history of

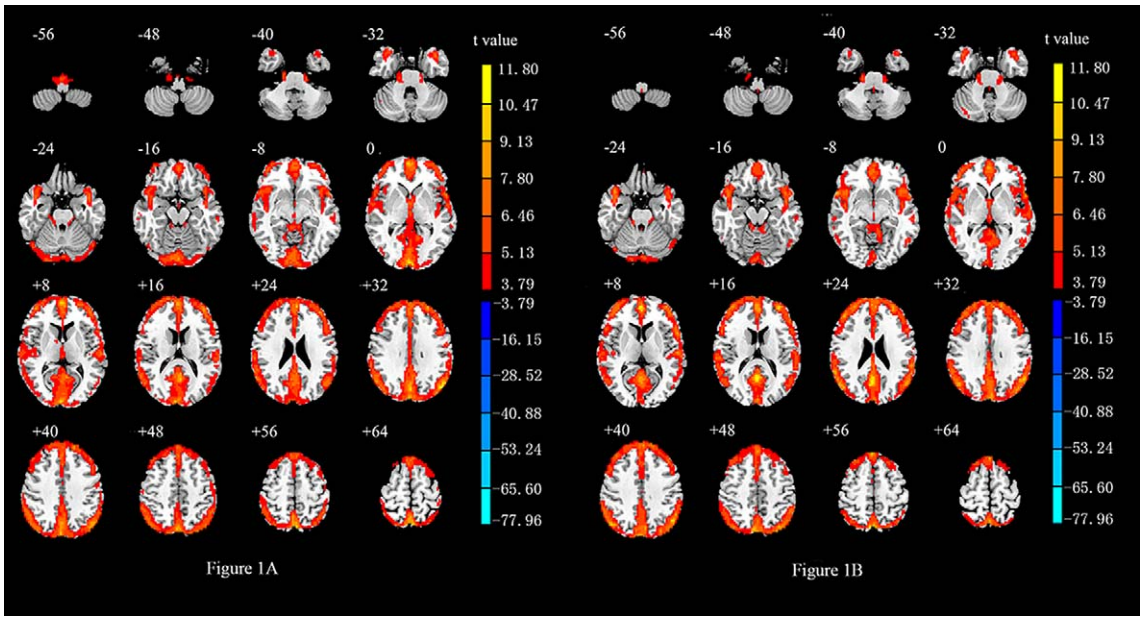

Figure 1. Results of ALFF across all healthy control subjects (**A**) and patients with POAG (**B**) in the resting state (one-sample *t*-test; $P < 0.05$, FDR correction).

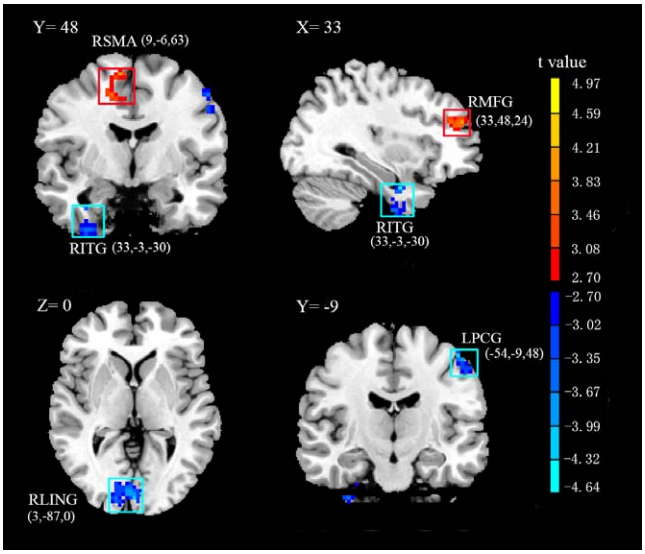

Figure 2. ALFF differences between POAG patients and healthy subjects. Compared with values in the control group, ALFF values in POAG patients increased in the right medial frontal gyrus (RMFG) and right supplementary motor area (RSMA), and decreased in the right occipital lingual gyrus (RLING), right inferior temporal gyrus (ITG), and left precentral gyrus. Threshold was set at $P < 0.01$ (AlphaSim corrected, $P < 0.05$, 54 voxels).

any significant medical, neurological, or psychiatric illness including hypertension and diabetes; (2) presence of ocular disease via a routine clinical ophthalmology test; and (3) use of alcohol, caffeine, or nicotine within the last 3 months. The clinical history of every patient was inquired about in detail. After recruitment into the study, all the patients signed an integrity agreement stating that they would not meet the exclusion criteria. On the other hand, all the healthy volunteers sighed the integrity agreement 3 months before the MRI scan.

All the glaucomatous eyes were classified using the Hodapp-Anderson-Parrish (HAP) system.[29] We consider the summation of the HAP grading scales of both eyes a HAP score for evaluating disease severity.

Data Acquisition

Magnetic resonance imaging data was acquired using a GE Signa HDxt 3.0T MRI scanner (General Electric Medical Systems, Milwaukee, WI, USA). For the resting-state scans, subjects were instructed simply to rest with their eyes closed, to relax but not to fall asleep. Head movements were prevented by a custom-built head holder. The images were parallel to the anterior commissure (AC)-posterior commissure (PC) line and covered the whole brain. The resting-state scan lasted 6 minutes 40 seconds and acquired 200 resting-state volumes. Twenty-eight axial slices were obtained using a T2*-weighted single-shot, gradient-recalled echo planar imaging sequence (FOV = 240 × 240 mm, matrix = 64 × 64, thickness = 5 mm, TR = 2000 ms, TE = 35 ms, flip angle = 90°). After the functional run, high-resolution structural information (3D-BRAVO) on each subject was also acquired using three-dimensional MRI sequences with a voxel size of 1 mm^3 for anatomical localization (TR = 8.8 ms, TE = 3.5 ms, matrix = 256 × 256, FOV = 240 × 240 mm, flip angle = 13°, slice thickness = 1 mm).

Data Preprocessing

Standard professional data processing software, Data Processing Assistant for Resting-State fMRI (DPARSF 2.1; State Key Laboratory of Cognitive Neuroscience and Learning, Beijing Normal University, Beijing, China; available in the public domain at http://restfmri.net/forum/DPARSF), was used for the data analysis. DPARSF is plug-in software running on a matrix laboratory platform (MATLAB R2012a; MathWorks, Inc., Natic, MA, USA) and is based on statistical parametric mapping (SPM; Wellcome Trust Centre for Neuroimaging, University College London, London, UK; available in the public domain at http://www.fil.ion.ucl.ac.uk/spm) and a resting-state fMRI data analysis toolkit (REST 1.8; Song et al., available in the public domain at http://www.restfmri.net).

The preprocessing steps were as follows. After converting DICOM files to NIFTI images, the first 10 time points were discarded. Slice timing and spatial realignment were then performed. We used a linear regression process to remove the effects of head motion and other possible sources of artifacts: (1) six motion parameters, (2) whole-brain signal averaged over the entire brain, (3) white matter signal, and (4) cerebrospinal fluid signal. The remaining data were then normalized to Montreal Neurological Institute (MNI) space by using echo planar imaging templates and resampling to 3-mm isotropic voxels. The linear trend of time courses was removed. Finally, the fMRI wave form of each voxel was temporally band-pass filtered (0.01–0.08 Hz).

Amplitude of Low-Frequency Fluctuation Analysis

Amplitude of low-frequency fluctuation analysis was calculated using the Resting-State fMRI Data Analysis Toolkit (http://www.restfmri.net). The time series of each voxel was transformed to the frequency domain using Fast Fourier Transform (FFT) (parameters: taper percent = 0, FFT length = shortest), and the power spectrum was obtained. Then the power spectrum obtained by FFT was square rooted and then averaged across 0.01 to 0.08 Hz at each voxel. This averaged square root was taken as ALFF. Fractional ALFF is the fraction of ALFF in a given

Table 2. Regions Showing ALFF Differences Between POAG Subjects and Healthy Controls

Brain Regions	BA	Voxels	MNI Coordinates, mm			*t*-Score for Peak Voxels
			x	*y*	*z*	
Right MFG	10	57	33	48	24	3.934
Right SMA	6	65	9	−6	63	3.9336
Right lingual gyrus	17/18	271	3	−87	0	−4.3535
Right ITG	37	60	33	−3	−30	−4.6129
Left PCG	4	55	−54	−9	48	−4.6382

BA, Brodmann's area; *x*, *y*, *z*, MNI coordinates of primary peak locations in the space of Talairach. Positive sign in the peak *t*-score represents increase, and negative sign represents decrease. The statistical threshold was set at $P < 0.01$, with AlphaSim corrected ($P < 0.05$, 54 voxels). The brain regions are shown in Figure 2.

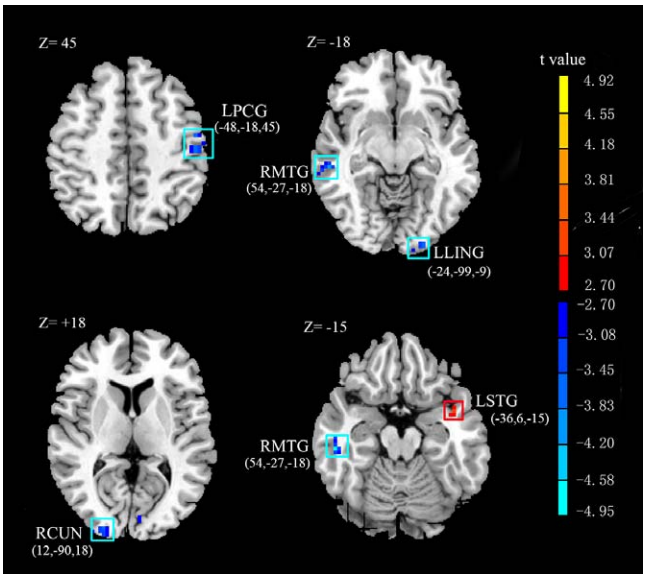

Figure 3. Fractional ALFF differences between POAG patients and healthy subjects for slow 4. Compared with the control group values, fALFF values in POAG patients decreased in the right middle temporal gyrus (MTG), left lingual gyrus (LLING), right cuneus (RCUN), and left postcentral gyrus (LPCG); and an increased fALFF value was seen in the left superior temporal gyrus (STG) for band slow 4 at $P < 0.01$ (AlphaSim corrected, $P < 0.01$, 16 voxels).

frequency band to the ALFF over the entire frequency range detectable in a given signal. As fALFF may be more robust against physiological noise, the low-frequency range for the BOLD signal was further decomposed into a slow 4 (0.027–0.073 Hz) and a slow 5 (0.01–0.027 Hz) band. Finally, the fALFF for slow 4 and slow 5 bands were calculated. For standardization purposes, the ALFF/fALFF of each voxel was divided by the global mean ALFF/fALFF value. Finally, all the ALFF/fALFF images were smoothed by a Gaussian kernel with a full width at half maximum of 4 mm.

Statistical Analysis

Statistical analysis utilized REST (http://www.restfmri.net). A one-sample *t*-test ($P < 0.05$, false discovery rate [FDR] correction) was performed to extract the ALFF results across the subjects within each group. Then we compared ALFF and fALFF for the slow 4 and slow 5 band results between POAG patients and healthy controls by performing a two-sample *t*-test. Finally, to further investigate the association between the ALFF abnormalities and the HAP grading scale of POAG patients, correlation analyses were carried out using REST with age and sex as covariates.

Results

Altered ALFF results across all subjects of the two groups during resting state are illustrated in Figure 1 ($P < 0.05$, FDR correction). The major regions of default-mode network (DMN) exhibited significant, higher ALFF values than other brain regions during the resting state, that is, the medial temporal lobe, posterior cingulate cortex (PCC), precuneus, medial prefrontal cortex, and inferior parietal lobule (IPL).

We then made a comparison between POAG patients and healthy controls to find the regions showing abnormal ALFF or fALFF values in POAG patients during the resting state. As shown in Figure 2, the results of a two-sample *t*-test revealed that POAG patients showed a significant ALFF value increase in the right middle frontal gyrus (MFG) and supplementary motor area (SMA), and a decrease in the right occipital lingual gyrus, right inferior temporal gyrus (ITG), and left postcentral gyrus (PCG) at $P < 0.01$ (AlphaSim corrected, $P < 0.05$, 54 voxels; Table 2). To compare with normal controls, we further investigated the abnormalities in fALFF of POAG patients for the slow 4 and slow 5 bands. The results revealed that POAG patients had decreased fALFF values in the right superior frontal gyrus (MTG), left lingual gyrus and cuneus, and right cuneus and left PCG, and an increased fALFF value in the left middle temporal gyrus (STG) for slow 4 band at $P < 0.01$ (AlphaSim corrected, $P < 0.01$, 16 voxels; Fig. 3; Table 3). They also had decreased fALFF values in the left PCC, left cuneus, right limbic lobe, and left PCG and increased fALFF values in the left IPL, right middle cingulate cortex (MCC), and right MFG for slow band 5 at $P < 0.01$ (AlphaSim corrected, $P < 0.05$, 30 voxels; Fig. 4; Table 4).

In addition, we investigated the correlation between ALFF and fALFF and HAP score. The results showed that the ALFF value of the right superior frontal gyrus (SFG) was positively correlated with HAP score and that the ALFF value of the left cuneus was negatively correlated with HAP score at $P < 0.01$ (AlphaSim corrected, $P < 0.05$, 30 voxels; Fig. 5; Table 5). For the slow 5 band, the fALFF values of bilateral MTG were negatively correlated with HAP score at $P < 0.01$ (AlphaSim corrected, $P < 0.05$, 30 voxels; Fig. 6; Table 6). There was no significant correlation between the fALFF values in the slow 4 band and the HAP score.

Discussion

In the current study, we measured ALFF values and fALFF values to assess the altered spontaneous neural activity in patients with POAG. Compared with controls, POAG patients had significantly decreased ALFF values in right occipital lingual gyrus, right ITG, and left precentral gyrus, and significantly increased ALFF values in right MFG and SMA. Meanwhile, POAG patients showed significantly decreased

Table 3. Regions Showing Difference in fALFF in Slow 4 Between the POAG Patients and Healthy Controls

Brain Regions	BA	Voxels	MNI Coordinates, mm			*t*-Score for Peak Voxels
			x	*y*	*z*	
Left STG	13/38	21	−36	6	−15	3.6916
Right MTG	21	28	54	−27	−18	−4.9546
Left lingual gyrus	17/18	16	−24	−99	−9	−3.53
Left cuneus	17/18	21	−9	−90	3	−4.4303
Right cuneus	18/19	63	12	−90	18	−4.2766
Left PCG	3/4	33	−48	−18	45	−4.0714

Positive sign in the peak *t*-score represents increase, and negative sign represents decrease. The statistical threshold was set at $P < 0.01$, with AlphaSim corrected ($P < 0.01$, 16 voxels). The brain regions are shown in Figure 3.

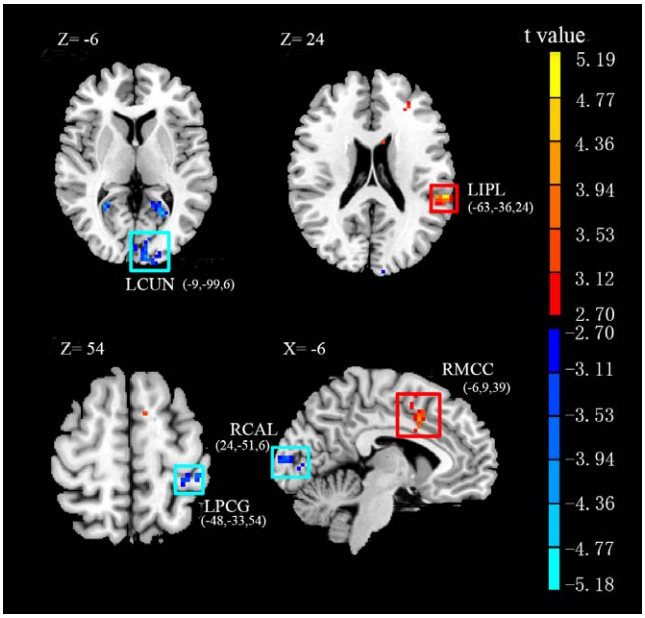

FIGURE 4. Fractional ALFF differences between POAG patients and healthy subjects for slow 5. Compared with the control group values, fALFF values in POAG patients degreased in cuneus of the left occipital lobe (LCUN) and left postcentral gyrus (LPCG), and increased in the left inferior parietal lobule (IPL) and right middle cingulate cortex (RMCC). Threshold was set at $P < 0.01$ (AlphaSim corrected, $P < 0.05$, 30 voxels).

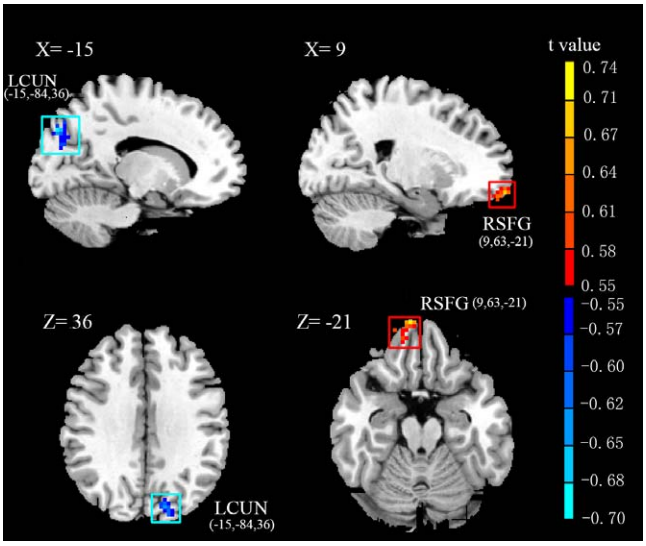

FIGURE 5. Correlations between ALFF and HAP scores. ALFF value of the right superior frontal gyrus (SFG) was positively correlated with HAP scores, and ALFF value of the left cuneus (LCUN) was negatively correlated with HAP scores. $P < 0.01$ (AlphaSim corrected, $P < 0.05$).

fALFF values in the bilateral cuneus, right MTG, PCG, left PCC, and right limbic lobe, and significantly increased fALFF values in the right MCC, left IPL, and right MFG. The results also showed that HAP stage was negatively correlated with the spontaneous neural activities in the left cuneus and bilateral MTG, and positively correlated with that in the right SFG.

Both ALFF and fALFF values were calculated in this study, since ALFF had higher test–retest reliability in previous studies while fALFF was verified to be less susceptible to physiological artifacts.[23] As ALFF bear similarities to fluctuations in neurophysiological, dynamic, and metabolic parameters,[30] those brain regions with decreased ALFF could suffer from dynamic and metabolic problems. In the study of fALFF, we used the slow 4 band (0.027–0.073 Hz) and slow 5 band (0.01–0.027 Hz),[31] since other bands of frequency mainly reflected noise rather than the physiological signal.[21] As certain brain regions may have varying sensitivity to different frequency bands,[32] we could get more information about the pattern of spontaneous neural activity in POAG patients with these two bands.

TABLE 4. Regions Showing Difference in fALFF in Slow 5 Between the POAG Patients and Healthy Controls

Brain Regions	BA	Voxels	MNI Coordinates, mm			*t*-Score for Peak Voxels
			x	*y*	*z*	
Left IPL	40	35	−63	−36	24	5.1854
Right MCC	32	78	−6	9	39	4.2131
Right MFG	9	39	−24	39	30	3.8876
Left PCG	3/2	30	−48	−33	54	−3.9936
Right calcarine/limbic lobe	23	33	24	−51	6	−4.1031
Left cuneus	17/18	110	−9	−99	6	−4.2655
Left calcarine/posterior cingulate	30	32	−24	−60	9	−5.183

Positive sign in the peak *t*-score represents increase, and negative sign represents decrease. The statistical threshold was set at $P < 0.01$, with AlphaSim corrected ($P < 0.05$, 30 voxels). The brain regions are shown in Figure 4.

TABLE 5. Regions Showing Significant Correlations Between ALFF and HAP Scores for the POAG Patients

Brain Regions	BA	Voxels	MNI Coordinates, mm			*r*-Score for Peak Voxels
			x	*y*	*z*	
Right SFG	11	47	9	63	−21	0.73632
Left cuneus	19/18	209	−15	−84	36	−0.7003

Positive *r*-score indicates positive correlation between the HAP score and the ALFF value, and negative *r*-score indicates negative correlation between the HAP score and the ALFF value. The statistical threshold was set at $P < 0.01$, with AlphaSim corrected ($P < 0.05$, 30 voxels). The brain regions are shown in Figure 5.

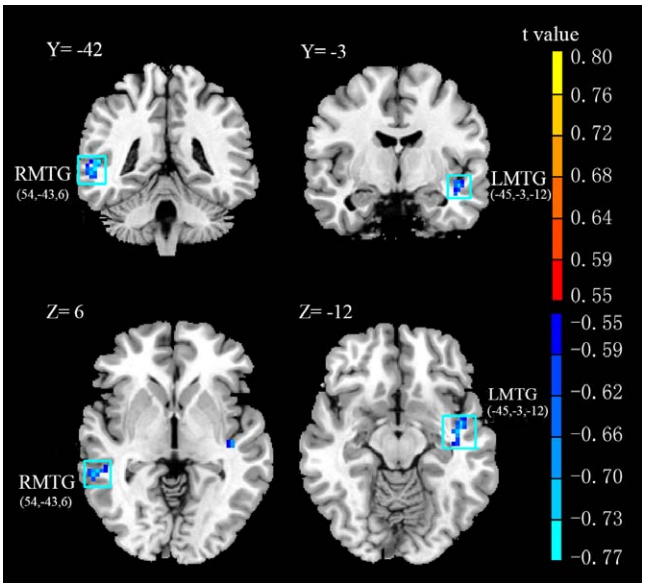

FIGURE 6. Correlations between fALFF for slow 5 and HAP scores. The fALFF values of bilateral MTG were negatively correlated with HAP scores. $P < 0.01$ (AlphaSim corrected, $P < 0.05$, 30 voxels).

In the present study, significantly decreased spontaneous neural activities were detected in visual cortices of POAG patients, including bilateral occipital lobe and right ITG. The lingual gyrus and cuneus of the occipital lobe are parts of Brodmann's area 17 (BA17), Brodmann's area 18 (BA18), and Brodmann's area 19 (BA19). Brodmann's area 17 is defined as the PVA that is directly connected with RGC. Brodmann's areas 8 and 19 are defined as higher visual cortices that receive input information from the PVA. When given visual stimulation, the PVA receives information from the lateral geniculate nucleus and then sends it out through two distinct anatomical streams.[33] The ITG is a component of the ventral stream, where the decreased spontaneous neural activity in this area might suggest dysfunction in visual stimuli processing, object identification, and memory recall. A reduction of spontaneous neural activity in these areas indicated that both primary and higher visual cortices are impaired. A recent study of regional homogeneity[34] and prior studies of proton magnetic resonance spectroscopy[35,36] led to a similar consequence. As the loss of RGCs and transsynaptic degeneration of the lateral geniculate nucleus are accepted as the mechanism of glaucoma,[37] transsynaptic degeneration and input reduction could be the main reasons for the dysfunction of visual cortices. In studies of optic neuritis, similar alterations of brain function were interpreted as a result of reduced neuronal input caused by edema, inflammation, later demyelination, and axonal loss.[38] The degeneration of synapse plays an important role in other neural degenerative diseases.[39,40] In prior research, the neural activity in visual cortex was also decreased in AD.[41] However, we cannot absolutely exclude the possibility of primary involvement, which might partly contribute to the hypometabolism. From these types of evidence, we catch a glimpse of the potential relationship between glaucoma and other neurodegenerative diseases.

The abnormalities were located not only in visual cortex, but also in the DMN, limbic system, and motor and sensory networks. This alteration of brain function is similar to that in other neurodegenerative diseases. Among these areas, the DMN is primarily concerned. The PCC, MTG, medial prefrontal cortex (MPFC), and IPL are major regions of the DMN. The PCC is considered the central node in the DMN, and the decreased ALFF of this area is tightly linked to AD progression in previous studies.[42–44] The hypometabolism and atrophy of medial temporal lobe in AD progression was also revealed.[45,46] In this study, significantly decreased fALFF values in the left PCC and right MTG were observed in POAG patients, and those in the right MFG and left IPL were significantly increased in POAG patients. These results were not totally the same as those of prior AD research, which showed decreased spontaneous neural activity in MPFC.[44,47] The difference could be due to differing progression of neurodegeneration. At an early stage of AD, the posterior cortical regions were the first to be affected, and other regions, including frontal cortex, were vulnerable at lower levels and later stages.[45] With respect to our results, the increased activity in anterior DMN areas could be interpreted as a compensatory process for decreased activity in posterior DMN areas.[48] Similar alterations in healthy elderly persons, mild cognitive impairment, and neuromyelitis optica have also been interpreted as compensatory.[48–50] In POAG patients, a significant decrease in fALFF was shown in the right limbic lobe while a significant increase of fALFF was shown in the right MCC. As parts of the limbic system, these areas are primarily responsible for emotion, behavior, and long-term memory. Although POAG patients have been reported to experience higher levels of emotional instability than controls,[9] it was unfortunate that the patients recruited in this study did not undergo psychological testing to confirm the correlation between the psychological abnormalities and the fALFF values. Moreover, in patients with POAG, a reduction of spontaneous neural activity could also be found in some motor and sensory cortices, including the left PCG and left precentral gyrus. The PCG and precentral gyrus constitute the motor and sensory networks[51]; and in previous studies, this network was reported to be associated with PVA spontaneous activity.[19] Furthermore, it was reported that this network would have decreased functional connectivity and reduced regional homogeneity in patients with POAG.[20,34] Our results provided further evidence for the alteration in these areas.

In the present study, more brain regions were detected in slow 5 band than in slow 4 band. The slow 5 band revealed abnormalities in the left PCC, right limbic lobe, left IPL, right MCC, right MFG, left PCG, and left cuneus. However, the slow 4 band showed alteration in the left MTG, left lingual gyrus, right cuneus, left PCG, and left cuneus. In other research, the slow 5 band and slow 4 band also appeared to have different

TABLE 6. Regions Showing Significant Correlations Between fALFF in Slow 5 and HAP Scores for the POAG Patients

Brain Regions	BA	Voxels	MNI Coordinates, mm			*r*-Score for Peak Voxels
			x	*y*	*z*	
Left MTG	22	75	−45	−3	−12	−0.757
Right MTG	22	35	54	−42	6	−0.74998

Positive *r*-score indicates positive correlation between the HAP score and the ALFF value, and negative *r*-score indicates negative correlation between the HAP score and the ALFF value. The statistical threshold was set at $P < 0.01$, with AlphaSim corrected ($P < 0.05$, 30 voxels). The brain regions are shown in Figure 6.

sensitivities for detecting abnormalities in the human brain.[52] Thus, we inferred that the slow 5 and slow 4 bands could reflect different constituents of spontaneous neural activity and reveal the abnormalities from different perspectives.

The HAP grading scale was commonly used in previous studies to evaluate the severity of POAG.[53,54] We found that the HAP score was negatively correlated with the spontaneous neural activities in the left cuneus and bilateral MTG. The spontaneous activity in the right prefrontal cortex was positively correlated with the HAP score. These data indicated that the abnormalities in the visual cortex and DMN were related to the progression of POAG. This could further support the theory that POAG is a neurodegenerative disease in the CNS. As functional alteration appears before organic changes, ALFF/fALFF might be a complementary index to help in diagnosing and monitoring the disease.

There are several limitations in the present study. Firstly, the patients recruited in this study did not undergo neuropsychological tests. Although some patients in the study complained of depression or insomnia, there was no quantitative evidence to evaluate their mental problems. Thus, despite the fact that the abnormalities detected in the DMN and visual cortex were similar to those in neurodegenerative disease, it is difficult to confirm whether these alterations are correlated with cognitive impairment. We believe that this problem will attract more attention in the future. Secondly, dysfunction of the dorsal stream was not obvious in our results. Whether its appearance is caused by the mechanism of glaucoma or other factors still needs further research.

In conclusion, alterations in ALFF/fALFF in the visual cortex, DMN, limbic system, and motor and sensory networks are present in POAG, indicating that it is a complex neurodegenerative disease that affects multiple brain networks. Moreover, the abnormal spontaneous neural activities in left cuneus, bilateral MTG, and right prefrontal cortex are correlated with glaucoma stage, suggesting that ALFF and fALFF might be complementary indicators for the disease.

Acknowledgments

Supported by high levels of health technical personnel in Beijing city under Grant 2011-1-047; the National Natural Science Foundation of China under Grants 81227901 and 81271557; and the Project for the National Key Basic Research and Development Program (973) under Grant 2011CB707700.

Disclosure: **T. Li**, None; **Z. Liu**, None; **J. Li**, None; **Z. Liu**, None; **Z. Tang**, None; **X. Xie**, None; **D. Yang**, None; **N. Wang**, None; **J. Tian**, None; **J. Xian**, None

References

1. Kwon YH, Fingert JH, Kuehn MH, Alward WL. Primary open-angle glaucoma. *New Engl J Med*. 2009;360:1113–1124.
2. Quigley HA. Open-angle glaucoma. *New Engl J Med*. 1993; 328:1097–1106.
3. Casson RJ, Chidlow G, Wood JP, Crowston JG, Goldberg I. Definition of glaucoma: clinical and experimental concepts. *Clin Experiment Ophthalmol*. 2012;40:341–349.
4. Tham YC, Li X, Wong TY, Quigley HA, Aung T, Cheng CY. Global prevalence of glaucoma and projections of glaucoma burden through 2040: a systematic review and meta-analysis. *Ophthalmology*. 2014;121:2018–2090.
5. Jindal V. Glaucoma: an extension of various chronic neurodegenerative disorders. *Mol Neurobiol*. 2013;48:186–189.
6. Pasquale LR, Loomis SJ, Kang JH, et al. CDKN2B-AS1 genotype-glaucoma feature correlations in primary open-angle glaucoma patients from the United States. *Am J Ophthalmol*. 2013;155: 342–353, e345.
7. Gupta N, Ang LC, de Tilly LN, Bidaisee L, Yucel YH. Human glaucoma and neural degeneration in intracranial optic nerve, lateral geniculate nucleus, and visual cortex. *Br J Ophthalmol*. 2006;90:674–678.
8. Gupta N, Yucel YH. Glaucoma as a neurodegenerative disease. *Curr Opin Ophthalmol*. 2007;18:110–114.
9. Pache M, Flammer J. A sick eye in a sick body? Systemic findings in patients with primary open-angle glaucoma. *Surv Ophthalmol*. 2006;51:179–212.
10. Yu L, Xie B, Yin X, et al. Reduced cortical thickness in primary open-angle glaucoma and its relationship to the retinal nerve fiber layer thickness. *PLoS One*. 2013;8:e73208.
11. Hernowo AT, Boucard CC, Jansonius NM, Hooymans JM, Cornelissen FW. Automated morphometry of the visual pathway in primary open-angle glaucoma. *Invest Ophthalmol Vis Sci*. 2011;52:2758–2766.
12. Boucard CC, Hernowo AT, Maguire RP, et al. Changes in cortical grey matter density associated with long-standing retinal visual field defects. *Brain*. 2009;132:1898–1906.
13. Zikou AK, Kitsos G, Tzarouchi LC, Astrakas L, Alexiou GA, Argyropoulou MI. Voxel-based morphometry and diffusion tensor imaging of the optic pathway in primary open-angle glaucoma: a preliminary study. *Am J Neuroradiol*. 2012;33: 128–134.
14. Chen WW, Wang N, Cai S, et al. Structural brain abnormalities in patients with primary open-angle glaucoma: a study with 3T MR imaging. *Invest Ophthalmol Vis Sci*. 2013;54:545–554.
15. Miki A, Nakajima T, Takagi M, Shirakashi M, Abe H. Detection of visual dysfunction in optic atrophy by functional magnetic resonance imaging during monocular visual stimulation. *Am J Ophthalmol*. 1996;122:404–415.
16. Duncan RO, Sample PA, Weinreb RN, Bowd C, Zangwill LM. Retinotopic organization of primary visual cortex in glaucoma: comparing fMRI measurements of cortical function with visual field loss. *Prog Retin Eye Res*. 2007;26:38–56.
17. Qing G, Zhang S, Wang B, Wang N. Functional MRI signal changes in primary visual cortex corresponding to the central normal visual field of patients with primary open-angle glaucoma. *Invest Ophthalmol Vis Sci*. 2010;51:4627–4634.
18. Fox MD, Raichle ME. Spontaneous fluctuations in brain activity observed with functional magnetic resonance imaging. *Nat Rev Neurosci*. 2007;8:700–711.
19. Wang K, Jiang T, Yu C, et al. Spontaneous activity associated with primary visual cortex: a resting-state FMRI study. *Cereb Cortex*. 2008;18:697–704.
20. Dai H, Morelli JN, Ai F, et al. Resting-state functional MRI: functional connectivity analysis of the visual cortex in primary open-angle glaucoma patients. *Hum Brain Mapp*. 2013;34: 2455–2463.
21. Zuo XN, Di Martino A, Kelly C, et al. The oscillating brain: complex and reliable. *Neuroimage*. 2010;49:1432–1445.
22. Logothetis NK, Pauls J, Augath M, Trinath T, Oeltermann A. Neurophysiological investigation of the basis of the fMRI signal. *Nature*. 2001;412:150–157.
23. Zou QH, Zhu CZ, Yang Y, et al. An improved approach to detection of amplitude of low-frequency fluctuation (ALFF) for resting-state fMRI: fractional ALFF. *J Neurosci Methods*. 2008; 172:137–141.
24. Biswal B, Yetkin FZ, Haughton VM, Hyde JS. Functional connectivity in the motor cortex of resting human brain using echo-planar MRI. *Magn Reson Med*. 1995;34:537–541.
25. Kopell N, Ermentrout GB, Whittington MA, Traub RD. Gamma rhythms and beta rhythms have different synchronization properties. *Proc Natl Acad Sci U S A*. 2000;97:1867–1872.
26. Buzsaki G, Draguhn A. Neuronal oscillations in cortical networks. *Science*. 2004;304:1926–1929.

27. Zhou G, Liu P, Wang J, et al. Fractional amplitude of low-frequency fluctuation changes in functional dyspepsia: a resting-state fMRI study. *Magn Reson Imaging*. 2013;31:996–1000.
28. Han Y, Lui S, Kuang W, Lang Q, Zou L, Jia J. Anatomical and functional deficits in patients with amnestic mild cognitive impairment. *PLoS One*. 2012;7:e28664.
29. Hodapp E, Parrish RK, Anderson DR. *Clinical Decisions in Glaucoma*. St. Louis, MO: Mosby-Year Book, Inc.; 1993:52–61.
30. Shmuel A, Leopold DA. Neuronal correlates of spontaneous fluctuations in fMRI signals in monkey visual cortex: implications for functional connectivity at rest. *Hum Brain Mapp*. 2008;29:751–761.
31. Han Y, Wang J, Zhao Z, et al. Frequency-dependent changes in the amplitude of low-frequency fluctuations in amnestic mild cognitive impairment: a resting-state fMRI study. *Neuroimage*. 2011;55:287–295.
32. Hutchison WD, Dostrovsky JO, Walters JR, et al. Neuronal oscillations in the basal ganglia and movement disorders: evidence from whole animal and human recordings. *J Neurosci*. 2004;24:9240–9243.
33. Goodale MA, Milner AD. Separate visual pathways for perception and action. *Trends Neurosci*. 1992;15:20–25.
34. Song Y, Mu K, Wang J, et al. Altered spontaneous brain activity in primary open angle glaucoma: a resting-state functional magnetic resonance imaging study. *PLoS One*. 2014;9:e89493.
35. Chan KC, So KF, Wu EX. Proton magnetic resonance spectroscopy revealed choline reduction in the visual cortex in an experimental model of chronic glaucoma. *Exp Eye Res*. 2009;88:65–70.
36. Zhang Y, Chen X, Wen G, Wu G, Zhang X. Proton magnetic resonance spectroscopy ((1)H-MRS) reveals geniculocalcarine and striate area degeneration in primary glaucoma. *PLoS One*. 2013;8:e73197.
37. Yucel Y, Gupta N. Glaucoma of the brain: a disease model for the study of transsynaptic neural degeneration. *Prog Brain Res*. 2008;173:465–478.
38. Kolappan M, Henderson AP, Jenkins TM, et al. Assessing structure and function of the afferent visual pathway in multiple sclerosis and associated optic neuritis. *J Neurol*. 2009;256:305–319.
39. Spires-Jones TL, Hyman BT. The intersection of amyloid beta and tau at synapses in Alzheimer's disease. *Neuron*. 2014;82:756–771.
40. Gabilondo I, Martinez-Lapiscina EH, Martinez-Heras E, et al. Trans-synaptic axonal degeneration in the visual pathway in multiple sclerosis. *Ann Neurol*. 2014;75:98–107.
41. Wang K, Liang M, Wang L, et al. Altered functional connectivity in early Alzheimer's disease: a resting-state fMRI study. *Hum Brain Mapp*. 2007;28:967–978.
42. Liu X, Wang S, Zhang X, Wang Z, Tian X, He Y. Abnormal amplitude of low-frequency fluctuations of intrinsic brain activity in Alzheimer's disease. *J Alzheimers Dis*. 2014;40:387–397.
43. Liang P, Xiang J, Liang H, Qi Z, Li K, Alzheimer's Disease NeuroImaging Initiative. Altered amplitude of low-frequency fluctuations in early and late mild cognitive impairment and Alzheimer's disease. *Curr Alzheimer Res*. 2014;11:389–398.
44. Wang Z, Yan C, Zhao C, et al. Spatial patterns of intrinsic brain activity in mild cognitive impairment and Alzheimer's disease: a resting-state functional MRI study. *Hum Brain Mapp*. 2011;32:1720–1740.
45. Buckner RL, Snyder AZ, Shannon BJ, et al. Molecular, structural, and functional characterization of Alzheimer's disease: evidence for a relationship between default activity, amyloid, and memory. *J Neurosci*. 2005;25:7709–7717.
46. Sorg C, Riedl V, Muhlau M, et al. Selective changes of resting-state networks in individuals at risk for Alzheimer's disease. *Proc Natl Acad Sci U S A*. 2007;104:18760–18765.
47. Xi Q, Zhao XH, Wang PJ, Guo QH, Yan CG, He Y. Functional MRI study of mild Alzheimer's disease using amplitude of low frequency fluctuation analysis. *Chinese Med J*. 2012;125:858–862.
48. Qi Z, Wu X, Wang Z, et al. Impairment and compensation coexist in amnestic MCI default mode network. *Neuroimage*. 2010;50:48–55.
49. Mevel K, Chetelat G, Eustache F, Desgranges B. The default mode network in healthy aging and Alzheimer's disease. *Int J Alzheimers Dis*. 2011;2011:535816.
50. Liu Y, Liang P, Duan Y, et al. Abnormal baseline brain activity in patients with neuromyelitis optica: a resting-state fMRI study. *Eur J Radiol*. 2011;80:407–411.
51. Damoiseaux JS, Rombouts SA, Barkhof F, et al. Consistent resting-state networks across healthy subjects. *Proc Natl Acad Sci U S A*. 2006;103:13848–13853.
52. Liu X, Wang S, Zhang X, Wang Z, Tian X, He Y. Abnormal amplitude of low-frequency fluctuations of intrinsic brain activity in Alzheimer's disease. *J Alzheimers Dis*. 2014;40:387–397.
53. Garaci FG, Bolacchi F, Cerulli A, et al. Optic nerve and optic radiation neurodegeneration in patients with glaucoma: in vivo analysis with 3-T diffusion-tensor MR imaging. *Radiology*. 2009;252:496–501.
54. Wang MY, Wu K, Xu JM, et al. Quantitative 3-T diffusion tensor imaging in detecting optic nerve degeneration in patients with glaucoma: association with retinal nerve fiber layer thickness and clinical severity. *Neuroradiology*. 2013;55:493–498.

Investigative Ophthalmology & Visual Science